

Drifter motion in the Gulf of Mexico constrained by altimetric Lagrangian coherent structures

M. J. Olascoaga,¹ F. J. Beron-Vera,¹ G. Haller,² J. Triñanes,³ M. Iskandarani,¹
E. F. Coelho,⁴ B. K. Haus,¹ H. S. Huntley,⁵ G. Jacobs,⁶ A. D. Kirwan Jr.,⁵
B. L. Lipphardt Jr.,⁵ T. M. Özgökmen,¹ A. J. H. M. Reniers,¹ and A. Valle-Levinson⁷

Received 7 November 2013; accepted 16 November 2013; published 9 December 2013.

[1] Application of recent geometric tools for Lagrangian coherent structures (LCS) shows that material attraction in geostrophic velocities derived from altimetry data imposed an important constraint to the motion of drifters from the Grand Lagrangian Deployment (GLAD) in the Gulf of Mexico. This material attraction is largely transparent to traditional Eulerian analysis. Attracting LCS acted as approximate centerpieces for mesoscale patterns formed by the drifters. Persistently attracting LCS cores emerged 1 week before the development of a filament resembling the “tiger tail” of the *Deepwater Horizon* oil slick, thereby anticipating its formation. Our results suggest that the mesoscale circulation plays a significant role in shaping near-surface transport in the Gulf of Mexico. **Citation:** Olascoaga, M. J., et al. (2013), Drifter motion in the Gulf of Mexico constrained by altimetric Lagrangian coherent structures, *Geophys. Res. Lett.*, *40*, 6171–6175, doi:10.1002/2013GL058624.

1. Introduction

[2] Mesoscale material patterns are commonly observed in satellite images of the Gulf of Mexico (GoM). A recent example is the *Deepwater Horizon* oil slick’s “tiger tail” described by Olascoaga and Haller [2012]. Despite considerable activity in recent years, these material patterns remain poorly understood, mainly because the time-dependent flows that sustain them involve complex dynamical interactions between processes at both mesoscales and submesoscales. Also, as these flows evolve rapidly in time, traditional Eulerian methods often fail to reveal material patterns.

Additional supporting information may be found in the online version of this article.

¹Rosenstiel School of Marine and Atmospheric Science, University of Miami, Miami, Florida, USA.

²Institute of Mechanical Systems, ETH Zurich, Zurich, Switzerland.

³Instituto de Investigaciones Tecnológicas, Universidade de Santiago de Compostela, Santiago, Spain.

⁴Physics Department, University of New Orleans, New Orleans, Louisiana, USA.

⁵School of Marine Science and Policy, University of Delaware, Newark, Delaware, USA.

⁶Naval Research Laboratory, Stennis Space Center, Mississippi, USA.

⁷Department of Civil and Coastal Engineering, University of South Florida, Gainesville, Florida, USA.

Corresponding author: M. J. Olascoaga, RSMAS/AMP, University of Miami, 4600 Rickenbacker Cswy., Miami, FL 33149, USA. (jolascoaga@rsmas.miami.edu)

©2013. American Geophysical Union. All Rights Reserved.
0094-8276/13/10.1002/2013GL058624

[3] Observations sufficiently dense to permit extraction of material patterns on multiple scales have been rare. To fill this void, more than 300 satellite-tracked near-surface drifting buoys were deployed in the northeastern GoM over roughly 1 week as part of the Grand Lagrangian Deployment (GLAD) in July 2012. The positions of the drifters from this unprecedented deployment were tracked for up to 6 months. (Further details relating to GLAD are provided in section S1 of the online supporting information.)

[4] Here we show that material attraction in geostrophic velocities derived from satellite altimetry data exerted an important constraint to GLAD drifter motion, thereby suggesting that near-surface transport in the GoM is significantly influenced by the mesoscale circulation.

[5] To reach this conclusion we apply recent geometric tools for Lagrangian coherent structures (LCS)—the concealed skeleton of material lines that shapes global transport [Peacock and Haller, 2013]. These tools enable objective (i.e., frame independent) and directly Lagrangian detection of LCS [Haller and Beron-Vera, 2012; Farazmand and Haller, 2013], and isolation of LCS cores [Olascoaga and Haller, 2012]. Attracting LCS (generalized unstable manifolds) form the centerpieces of material patterns. LCS cores (generalized saddle points) are characterized by persistent material attraction and represent precursors of material instabilities.

[6] In the analysis we consider daily mean positions of GLAD drifters in two groups (of 90 drifters each) deployed 4 days apart at nearby locations, indicated by triangles in Figure 1(left). Focus is placed on the 20 days following the deployment of the first of these groups (22 July 2012). The large number of drifters and the low dispersion during this period allow one to easily distinguish the formation of patterns in their distributions.

[7] Ten days prior to the first deployment date, a long chlorophyll plume extending southeastward from the Mississippi River mouth was evident, as revealed in the satellite ocean color image shown in Figure 1(left). Plumes like this occur regularly, possibly strongly influenced by the evolving mesoscale field [Morey et al., 2005], which is dominated by the episodic shedding of Loop Current rings [Forristall et al., 1992]. The centerpiece of the chlorophyll plume is well represented by attracting LCS (black curves) extracted from altimetry using the methodology described below. This confirms the role attributed to the mesoscale circulation. Connections between the altimetric LCS and sea surface temperature (SST) fronts are more tentative (Figure 1, right). This is, to a large extent, a result of significant surface heating of the Gulf of Mexico during the summer months, so that SST is not a good

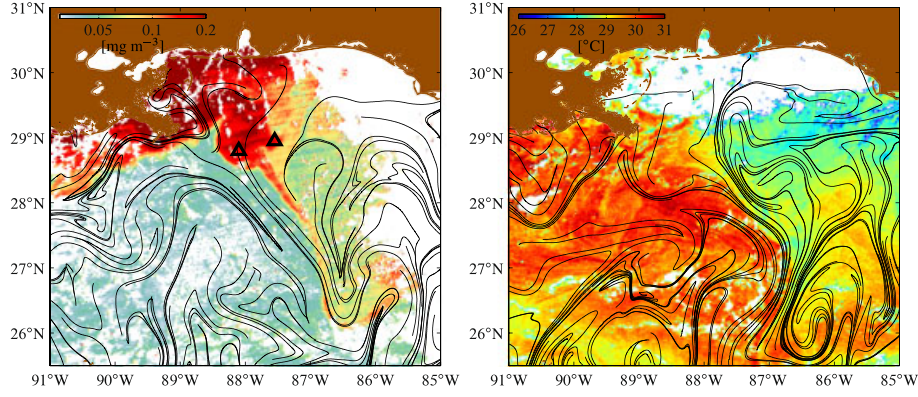


Figure 1. (left) Chlorophyll a concentration in the northern Gulf of Mexico on 12 July 2012 derived from the MODIS (Moderate Resolution Imaging Spectroradiometer) sensor aboard satellite *Aqua* with deployment sites in the two GLAD drifter groups considered indicated (triangles) and altimetric attracting LCS computed as 30 day backward squeezelines overlaid (black curves). (right) Sea surface temperature on 28 July 2012 derived from Advanced Very High Resolution Radiometer (AVHRR/3) sensor aboard satellite *NOAA-19* with LCS overlaid.

proxy for a passive tracer during this time of the year. Similar good correspondence is found between altimetric LCS and patterns acquired by GLAD drifters in the aforementioned groups.

2. Methods

[8] Consider an incompressible two-dimensional velocity field $v(x, t)$, where position x ranges on some domain of the plane and time t is defined on the finite interval $[\alpha, \beta]$. An often used objective measure of material deformation is the Cauchy-Green strain tensor,

$$C_{t_0}^t(x_0) := DF_{t_0}^t(x_0)^\top DF_{t_0}^t(x_0), \quad (1)$$

where $F_{t_0}^t(x_0) := x(t; x_0, t_0)$ is the advection map that associates times t_0 and t positions of fluid particles, which evolve according to

$$\dot{x} = v(x, t). \quad (2)$$

A local normal growth measure of the unit normal, n_0 , along a material line at time t_0 is given by the *normal repulsion rate* [Haller, 2011]:

$$\rho_{t_0}^t(x_0) := \frac{1}{\sqrt{n_0 \cdot C_{t_0}^t(x_0)^{-1} n_0}}. \quad (3)$$

Let $0 < \lambda_1(x_0) < \lambda_2(x_0) \equiv \lambda_1(x_0)^{-1}$ and $\xi_1(x_0) \perp \xi_2(x_0)$ (dependencies on t_0 and t are omitted for simplicity) be eigenvalues and (normalized) eigenvectors of (1). It follows that $\rho_{t_0}^t(x_0) = \sqrt{\lambda_2(x_0)} > 1$ [respectively, $\rho_{t_0}^t(x_0) = \sqrt{\lambda_1(x_0)} < 1$] for fluid particle trajectories whose t_0 positions form a material line along which $n_0 = \xi_2(x_0)$ [respectively, $n_0 = \xi_1(x_0)$]. Accordingly, a material line everywhere tangent to $\xi_1(x_0)$ [respectively, $\xi_2(x_0)$] is referred to as a *squeezeline* [respectively, *stretchline*].

[9] Detection of attracting LCS over the time interval $[\alpha, \beta]$ is achieved at any t_0 within this interval as follows. Attracting LCS at $t_0 = \beta$ are identified with locally most squeezing squeezelines at $t_0 = \beta$ obtained from backward computation out to $t = \alpha$ [Haller and Beron-Vera, 2012]. Attracting LCS at $t_0 = \alpha$ are identified with locally most stretching stretchlines at $t_0 = \alpha$ obtained from forward computation out to $t = \beta$ [Farazmand and Haller, 2013].

Attracting LCS at any $\alpha < t_0 < \beta$ are obtained from backward [respectively, forward] advection of attracting LCS at $t_0 = \beta$ [respectively, $t_0 = \alpha$].

[10] LCS cores are segments of attracting LCS that experience persistent, as opposed to just overall, attraction over the time interval $[\alpha, \beta]$ [Olascoaga and Haller, 2012]. Specifically, at $t_0 = \beta$ an LCS core is given by the $t_0 = \beta$ positions of fluid particles such that (3) monotonically increases from $t_0 = \beta$ to $t = \alpha$ (for more details, cf., section S2 of the online supporting information).

[11] The velocity field in (2) is assumed to be of the form

$$v(x, t) = gf(x_2)^{-1} \nabla^\perp \eta(x, t) + \nabla \varphi(x, t), \quad (4)$$

where g is the acceleration of gravity; $f(x_2)$ is the latitude-dependent Coriolis parameter; $\eta(x, t)$ is the sum of a mean dynamic topography and the altimetric SSH anomaly distributed by AVISO (Archiving, Validation, and Interpretation of Satellite Oceanographic data); and $\varphi(x, t)$ is such that the normal projection of $v(x, t)$ at the coastline vanishes (details on the altimetric data set and the computation of $\varphi(x, t)$ are provided in section S3 of the online supporting information).

[12] All integrations involved in the LCS analysis described below are carried out using a stepsize-adapting fourth-order Runge-Kutta method. Interpolations are obtained using a cubic scheme. Differentiation in (1) is executed using finite differences on an auxiliary 0.1 km width grid of four points neighboring each point in a regular 0.5 km width grid covering the domain of interest.

[13] The GLAD drifters followed the CODE (Coastal Ocean Dynamics Experiment) design [Davis, 1985]. The drifters were drogued at 1 m depth and tracked using GPS (Global Positioning System) with an accuracy of about 5 m and positions recorded nominally every 5 min. The raw drifter data were treated to remove outliers and fill occasional gaps, and also low-pass filtered with a 15 min cutoff. Our analysis uses daily mean drifter positions.

3. Results

[14] Figure 2 shows a sequence of snapshots of the evolution of GLAD drifters in the two groups of drifters noted

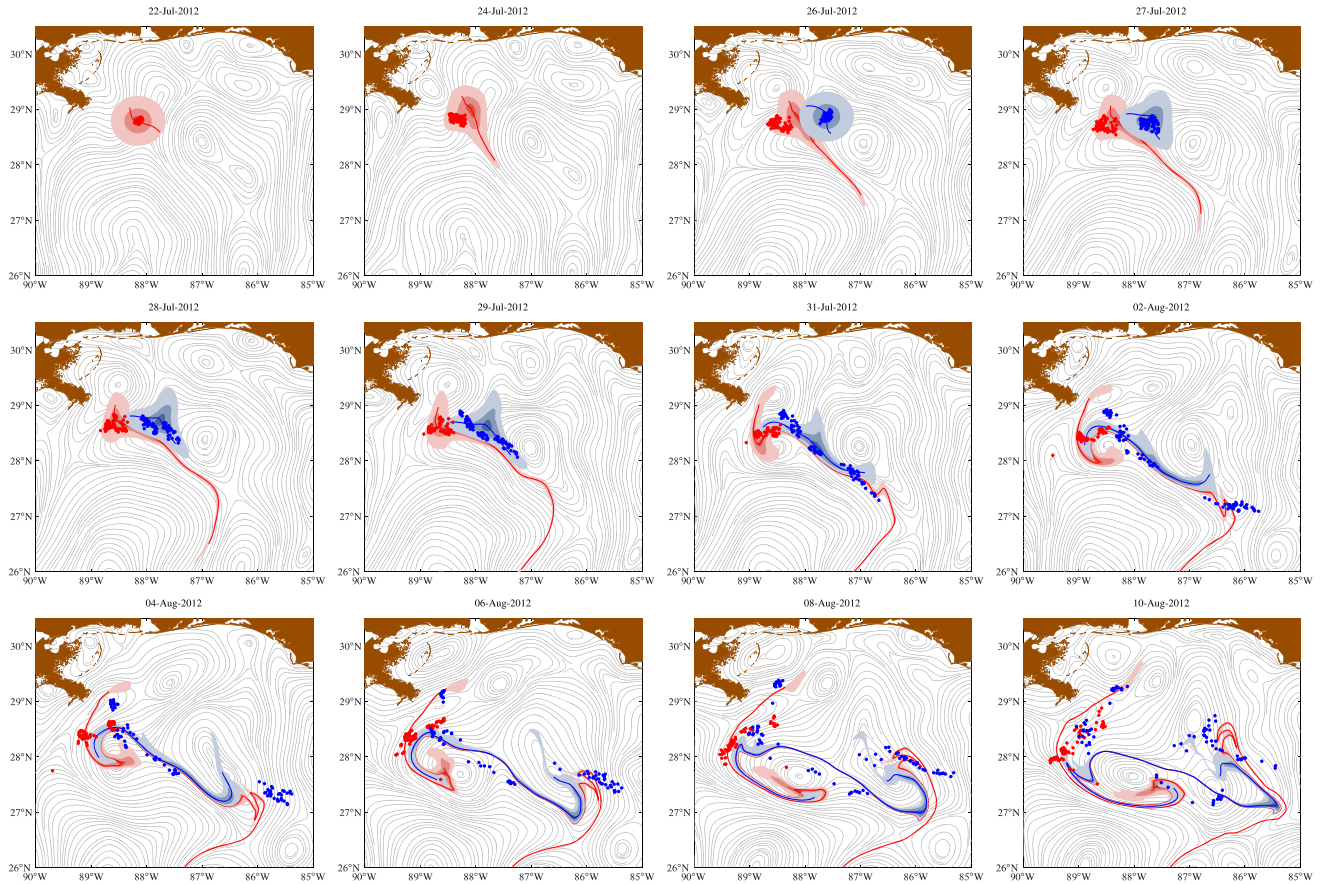


Figure 2. Sequence of selected snapshots of the evolution of fluid patches as advected by the altimetry-derived velocity field (4) (red and blue areas) and corresponding centerpieces or attracting LCS obtained as the advected images of forward stretchlines through the patches at the initial time (red and blue curves). Also indicated are S1 (red dots), S2 (blue dots) drifter positions, and instantaneous streamlines of the altimetry-derived velocity field (gray curves).

earlier. Drifters in the group deployed on 22 July 2012, denoted S1, are shown as red dots, while drifters in the group deployed 4 days later, denoted S2, are shown as blue dots. Several aspects of the motion of the drifters are worth noting. First, S1 drifters take a few days before they begin to spread and form a discernible pattern. This pattern is clearly evident only after 7 August 2012, when a roughly 100 km long filament is observed. Second, in marked contrast, S2 drifters spread and form a clear pattern rather quickly after deployment. Indeed, by 1 August 2012, S2 drifters have organized into a long filament of more than 200 km. This resembles quite well the “tiger tail” fingering instability of the oil slick during the *Deepwater Horizon* spill [Olascoaga and Haller, 2012; Huntley et al., 2011]. Finally, in addition to organizing into filaments, both S1 and S2 drifters exhibit some degree of clustering. This is evident, for instance, during the formation of the long filament by S2 drifters, which do not cover the filament uniformly.

[15] Figure 2 also shows, in gray, instantaneous streamlines of the altimetry-derived velocity field (4) and, in red and blue, snapshots of the evolution of two patches of fluid as advected by this field. Each patch is initially circular, centered at the deployment site of each drifter group on the corresponding deployment date. The color convention is the same as that for the drifters. The curve through each patch in each snapshot is an attracting LCS obtained as the advected image of the forward stretchline passing through the

center of the patch on the drifter deployment date. Stretchlines were obtained from forward integration out to 10 August 2012 from the respective deployment date. As expected, the LCS through each patch forms its organizing backbone, providing an explanation for the shapes acquired by the patches as time progresses. Identifying this from visual inspection of the instantaneous streamlines of the altimetry-derived velocity field is not trivial.

[16] The extent to which altimetric LCS constrain drifter motion can be assessed by comparing the patterns acquired by the drifters with those suggested by the extracted attracting LCS. Quick inspection reveals reasonable overall agreement between drifter and altimetric LCS evolution. Closer inspection reveals that the LCS initialized in the S1 deployment (red curve) does not form the centerpiece of the distributions acquired by the drifters over the initial 15 days of evolution. This LCS suggests faster spreading than that experienced by the drifters. Only during the last 5 days of evolution there is a tendency of the drifters to organize in a direction suggested by the LCS. In marked contrast, S2 drifters develop patterns generally in quite good agreement with those suggested by the LCS initialized in the S2 deployment (blue curve). This is most clearly evident over the first 5 days or so of evolution, which is characterized by the organization of the drifters into a long filament. The centerpiece of this filament is very well approximated by the LCS. This LCS cannot be claimed to form as clearly the centerpiece of

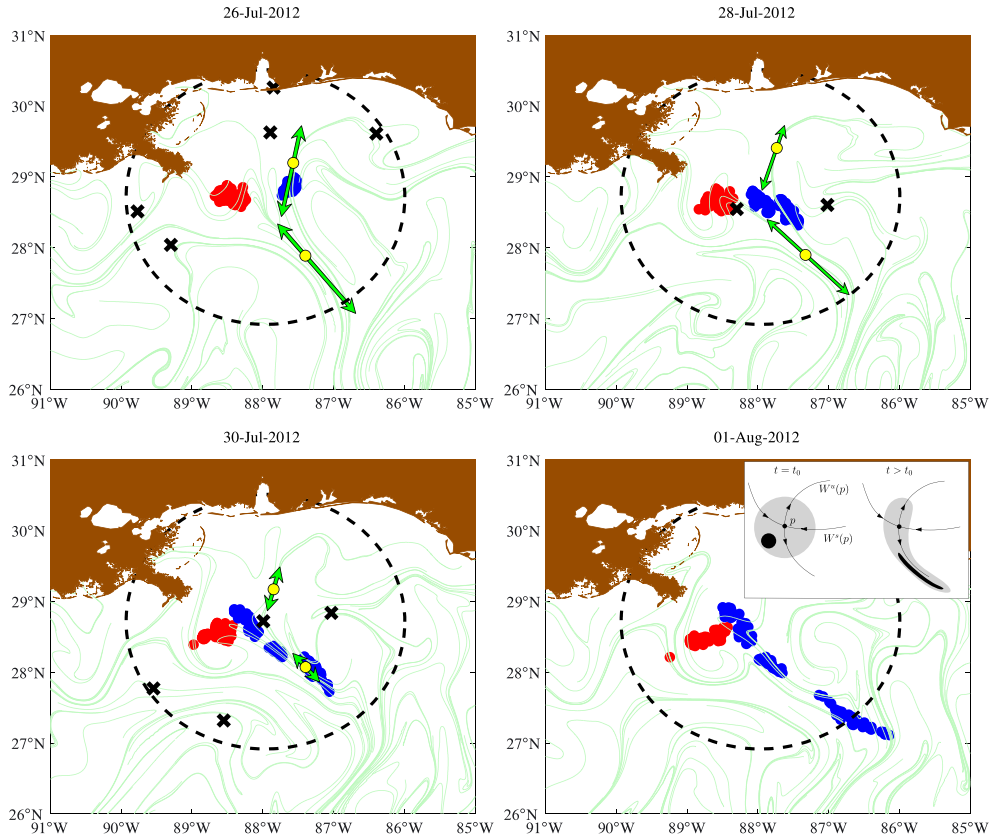


Figure 3. Altimetric LCS cores found within the circular domain delimited by the dashed line (yellow dots with green arrows attached); S1 (red dots) and S2 (blue dots) drifter positions; altimetric LCS computed as backward squeezelines (light green curves); and instantaneous saddle points of the altimetry-derived velocity field (black crosses). The inset in the lower right panel illustrates the effect of a saddle point on a material patch in steady flow. The saddle point, denoted p , is the counterpart of LCS core and the stable [respectively., unstable] manifold, denoted $W^s(p)$ [respectively, $W^u(p)$], is the counterpart of repelling [respectively, attracting] LCS.

the drifter patterns beyond 5 days. However, the drifters do follow to some extent the northward folding of the eastern end of the LCS. This is not true for the southward folding of the western end of the LCS, which is not accompanied by the motion of the drifters. But the drifters do appear to organize along the red LCS, initialized in the S1 deployment. Finally, the tendency of both S1 and S2 drifters to cluster is not described by the evolution of altimetric LCS.

[17] In view of the rather poor spatiotemporal resolution of the altimetry data set (with no more than 10 altimetry tracks on average per week covering the entire Gulf of Mexico), the agreement found between altimetric LCS and drifter motion is remarkable. The noted disagreements may well be a consequence of the coarseness of this data set, or the dynamics substantively deviating from quasigeostrophic at the unresolved scales. While shipboard wind measurements acquired during GLAD suggest that the Ekman drift is negligible, inertial oscillations are known to be important, and other ageostrophic motions such as those due to internal wave interaction with the bottom topography, and mixed layer and frontal instabilities may be at work too. Accounting for all these factors may help explain the differences in behavior between S1 and S2 drifters (the latter were deployed over the Desoto Canyon on a salinity front). The additional consideration of buoyancy and finite size effects may be needed to explain the

observed tendency of the drifters in each group to cluster [Provenzale, 1999].

[18] We now proceed to show that the organization of S2 drifters into a long filament can be anticipated by emerging LCS cores in the altimetry record, illustrating the predictive skill of LCS-core analysis (Figure 3). This is done by identifying LCS cores from attracting LCS at each assessment time t_0 , which are computed as most squeezing squeezelines obtained from backward integration over a period of 1 week. The search for developing LCS cores is restricted to a circular region of radius 200 km containing S2 drifters (LCS cores outside this region lie too far away from the drifters to influence their motion). Particular attention is paid to LCS cores that persist over time as these can more effectively accumulate momentum and hence more significantly affect the motion of the drifters. Each LCS core found is represented by a dot, indicating the position x_0^* where the backward normal repulsion rate, $\sqrt{\lambda_2(x_0)}$, is maximized. Attached to each dot are opposing arrows, indicating the plus and minus backward squeezing directions at x_0^* , $\pm \xi_1(x_0^*)$. The magnitude of each arrow is scaled by $\sqrt{\lambda_2(x_0)}$ averaged over points x_0 on the LCS core on each side of x_0^* . The preferred direction of stretching past the assessment time is suggested by that of the longest resulting arrow.

[19] Figure 3 shows two LCS cores that can be traced over time from 26 July 2012 out to 1 August 2012. These

LCS cores gradually lose strength over this period of time, with the northern LCS core doing so at a somewhat faster rate than the southern LCS core. Both LCS cores suggest asymmetric material spreading, with the preferred direction of spreading being southward. Accordingly, the northern LCS core is seen to be responsible for the initial southeastward motion of the drifters in group S2. This southeastward spread is enhanced by the action of the southern core when the drifters approach its area of influence, sometime between 28 and 30 July 2012. This is accompanied by some northwestward spreading resulting from the action of the southern LCS core. By 1 August 2012 the drifters in group S2 stretch out, delineating a long filament. Thus, similar to *Olascoaga and Haller* [2012], who related the formation of the *Deepwater Horizon* oil slick's "tiger tail" to the emergence of an LCS core a week before its development, the organization of S2 drifters into this filament is inferred about a week in advance by the emergence of the two LCS cores discussed above. We emphasize that this inference relies exclusively on velocity data up to the assessment time: no velocity forecast of any kind is needed. We finally note that instantaneous saddle points provide no indication about the location, direction, or magnitude of the LCS cores, making the conclusions from LCS core analysis unreachable from traditional Eulerian analysis.

4. Conclusions

[20] We have shown that material attraction in geostrophic velocities derived from altimetry data imposed an important constraint to the motion of GLAD drifters, which suggests a significant role for the mesoscale circulation in shaping near-surface transport in the GoM. While largely transparent to traditional Eulerian analysis, this conclusion was reached using recent geometric tools that enable objective and directly Lagrangian detection of LCS as well as persistently attracting LCS cores. Lack of resolution of the altimetry data set, ageostrophic effects, and buoyancy and

finite size effects are among possible causes for disagreement between altimetric LCS and drifter motion.

[21] **Acknowledgments.** We thank A. Poje for helpful comments and S. Chinchilla for proof reading an earlier version of the manuscript. S. Schofield was responsible for drifter electronics optimization. The altimetry data set is distributed by AVISO (<http://www.aviso.oceanobs.com>). Support for this work was provided by a BP/The Gulf of Mexico Research Initiative grant; NSF grant CMG0825547; NASA grant NX10AE99G; ONR grants N00014-10-1-0522, N00014-11-10081, and N00014-11-1-0087; and the Mary A. S. Lighthipe endowment at the University of Delaware.

[22] The Editor thanks two anonymous reviewers for their assistance in evaluating this paper.

References

- Davis, R. (1985), Drifter observations of coastal surface currents during CODE: The method and descriptive view, *J. Geophys. Res.*, *90*, 4741–4755.
- Farazmand, M., and G. Haller (2013), Attracting and repelling Lagrangian coherent structures from a single computation, *Chaos*, *23*, 023101.
- Forristall, G. Z., K. J. Schaudt, and C. K. Cooper (1992), Evolution and kinematics of a Loop Current eddy in the Gulf of Mexico during 1985, *J. Geophys. Res.*, *97*, 2173–2184.
- Haller, G. (2011), A variational theory of hyperbolic Lagrangian coherent structures, *Physica D*, *240*, 574–598, doi:10.1016/j.physd.2010.11.010.
- Haller, G., and F. J. Beron-Vera (2012), Geodesic theory of transport barriers in two-dimensional flows, *Physica D*, *241*, 1680–1702, doi:10.1016/j.physd.2012.06.012.
- Huntley, H. S., B. L. Lipphardt, and A. D. Kirwan (2011), Surface drift predictions of the Deepwater Horizon Spill: The Lagrangian perspective, in *Monitoring and Modeling the Deepwater Horizon Oil Spill: A Record-Breaking Enterprise*, *Geophys. Monogr. Ser.*, vol. 195, edited by Y. Liu et al., pp. 179–195, AGU, Washington, D. C., doi:10.1029/2011GM001097.
- Morey, S. L., J. Zavala-Hidalgo, and J. J. O'Brien (2005), The seasonal variability of continental shelf circulation in the northern and western Gulf of Mexico from a high-resolution numerical model, in *Circulation in the Gulf of Mexico: Observations and Models*, *Geophys. Monogr. Ser.*, vol. 161, edited by W. Sturges and A. Lugo-Fernandez, pp. 203–218, AGU, Washington, D. C., doi:10.1029/161GM16.
- Olascoaga, M. J., and G. Haller (2012), Forecasting sudden changes in environmental pollution patterns, *Proc. Nat. Acad. Sci. U.S.A.*, *109*, 4738–4743.
- Peacock, T., and G. Haller (2013), Lagrangian coherent structures: The hidden skeleton of fluid flows, *Phys. Today*, *66*, 41–47.
- Provenzale, A. (1999), Transport by coherent barotropic vortices, *Annu. Rev. Fluid Mech.*, *31*, 55–93.